NATIONAL ADVISORY COMMITTEE FOR AERONAUTICS

TECHNICAL NOTE 2769

EXPERIMENTAL AND THEORETICAL DETERMINATION OF THERMAL STRESSES IN A FLAT PLATE

By Richard R. Heldenfels and William M. Roberts

Langley Aeronautical Laboratory
Langley Field, Va.

Washington
August 1952

1A

NATIONAL ADVISORY COMMITTEE FOR AERONAUTICS

TECHNICAL NOTE 2769

EXPERIMENTAL AND THEORETICAL DETERMINATION OF THERMAL STRESSES IN A FLAT PLATE

By Richard R. Heldenfels and William M. Roberts

SUMMARY

Thermal stresses induced in a flat, rectangular, 75S-T6 aluminum-alloy plate by nonuniform heating are determined both experimentally and theoretically. The characteristics of commercially available bonded resistance wire strain gages are first investigated to determine their suitability for measuring stresses under simple conditions of stress and temperature. The gages are then used to measure thermal stresses in the flat plate in order to study their suitability under more complicated conditions. The experimental results are found to be in satisfactory agreement (within ±5 percent of the maximum calculated stress) with an approximate theoretical solution of the problem.

INTRODUCTION

Aerodynamic heating of aircraft flying at supersonic speeds has become important in structural design because material properties are changed by exposure to elevated temperatures, and thermal stresses which result from nonuniform heating may have a significant effect on the strength of the structure. Methods for determining thermal stresses are therefore required if an efficient design is to be attained.

References 1 and 2 considered the thermal-stress problem in aircraft structures theoretically and presented some procedures for thermal-stress analysis. The methods presented varied in their accuracy and involved various assumptions and approximations. These theoretical approaches alone, therefore, are not sufficient, and experimental methods are needed to check the accuracy of approximate thermal-stress-analysis procedures and to help analyze those structures which are too complex for theoretical analysis.

An investigation has therefore been made of the characteristics of commerically available bonded resistance wire strain gages to determine their suitability for measuring stresses under simple conditions of

stress and temperature, and the results are presented in this paper. The strain gages are used to measure the thermal stresses induced in a flat plate subject to a known, nonuniform temperature distribution to study their suitability under more complicated conditions. The stresses so measured are then compared with an approximate theoretical solution, the details of which are included in the appendix.

SYMBOLS

a	half-length of plate, in.
b	half-width of plate, in.
E	modulus of elasticity, psi
E_0	modulus of elasticity at room temperature, psi
T	temperature, $^{\circ}F$
T_0	temperature at which thermal stresses are assumed to be zero, $^{\circ}F$
T_1	temperature difference between center line and longitudinal edge of plate, $^{\circ}F$
U	strain energy, in.-lb
x, y	coordinate axes
α	coefficient of thermal expansion, $\frac{\text{in.}}{\text{in.}-^{\circ}F}$
ϵ	total-strain reading of gage, in./in.
ϵ'	net strain, $\epsilon - \lambda$, in./in.
λ	zero shift of strain gage due to temperature changes, in./in.
μ	Poisson's ratio
σ_x	longitudinal direct stress, psi
σ_y	transverse direct stress, psi
τ_{xy}	shear stress, psi

Φ stress function

∇^2 differential operator, $\frac{\partial^2}{\partial x^2} + \frac{\partial^2}{\partial y^2}$

∇^4 differential operator, $\frac{\partial^4}{\partial x^4} + 2\frac{\partial^4}{\partial x^2 \partial y^2} + \frac{\partial^4}{\partial y^4}$

STRAIN-GAGE CHARACTERISTICS

An ideal strain gage, when mounted on a test specimen, would produce stable, accurate, and reproducible readings under all conditions of stresses and temperatures. That is, the reading would not drift under constant stress and temperature, the reading would be unique for each combination of stress and temperature, and the reading would be the same for different gages of the same type. If such a gage were available, the measured strain might be simply related to a uniaxial stress in the elastic range as follows:

$$\sigma = E\epsilon' = E(\epsilon - \lambda)$$

where

σ stress, psi

E modulus of elasticity of the specimen which is a function of temperature, psi

ϵ' net strain, in./in.

ϵ measured strain, in./in.

λ zero shift due to temperature change, in./in. (called zero shift because it is the measured strain due to temperature changes under zero stress conditions)

If bonded resistance wire strain gages could closely approximate such behavior, they would provide a simple means of measuring thermal stresses. A study was therefore made to determine the characteristics of one type of wire strain gage and its suitability for measuring thermal stresses.

Commercially available Baldwin SR-4 type AB-7 strain gages were selected for investigation. These $\frac{1}{4}$-inch-gage-length bakelite gages

were chosen because of their good elevated-temperature characteristics (ref. 3) and because subsequent tests required a short gage length. The AB-7 gage was selected in preference to self-compensating gages because the latter were not available in sufficient quantity when this study was undertaken. The higher cost of the self-compensating gages also discourages their use when large numbers of gages such as were used herein are needed.

The characteristics of the AB-7 gages were studied at temperatures between 80° F and 300° F and at various stress levels in the elastic range of 75S-T6 aluminum alloy. The study was carried out by mounting a gage on each side of a 75S-T6 aluminum-alloy block. The gages were mounted in accordance with procedures recommended by the manufacturer and were read separately on a type K Baldwin SR-4 strain indicator. A pure compression load was applied to the block by means of a hydraulic testing machine and temperatures were controlled by an electric furnace (ref. 4). Throughout these and all subsequent tests, a consistent wiring arrangement was used so that wiring effects would be included in the calibration.

The specimen and the mounted gages were first exposed to conditions of constant stress and temperature to investigate the stability of the gages — that is, to find whether the gage reading changed with time and, if so, how much it changed. Changes of 10 microinches per inch, probably due to creep of the gage and specimen, were detected for exposures of approximately 1/2 hour at 300° F and 12 ksi but were considered small enough to be neglected for this condition and for longer times at lower stresses and temperatures. The gages are thus deemed sufficiently stable for short-time tests.

Accuracy and reproducibility were next investigated by obtaining compressive stress-strain curves in the elastic range for temperatures up to 300° F. Figure 1 shows typical stress-strain curves at three temperatures for an AB-7 gage mounted on 75S-T6 aluminum alloy. The curves of figure 1 were obtained by measurement in the compression range and extrapolation into the tension range by assuming that the modulus of elasticity is the same for tension and compression. The curves of figure 1 are defined by two quantities: the slope of each line, which is actually the modulus of elasticity of the specimen, and the spacing along the horizontal axis, which is the zero shift.

The ratio of the modulus of elasticity of 75S-T6 aluminum alloy at the test temperature to its modulus at room temperature, both measured by the AB-7 gages, is plotted in figure 2. Included in the figure are the average values and scatter band of the modulus ratio of 75S-T6 aluminum alloy as determined by a different method and reported in reference 4. The modulus ratios obtained by means of AB-7 gages are seen to be within the accuracy of those of reference 4 and the gage factor is apparently

constant. Reference 3 also found that the gage factor of AB-7 gages was constant in this temperature range. Reproducibility was indicated since different gages gave substantially the same modulus ratios.

The zero shift differed from gage to gage on the same specimen and was dependent upon the previous temperature history of the gage. The response of a particular gage to temperature changes was found, however, to become fairly consistent if the gages were mounted, cured at a temperature above that at which they were to be used, and then put through several temperature cycles. Even after this treatment, however, the responses varied from gage to gage within the range shown in figure 3. The data of figure 3 were obtained from 70 of the 72 different gages used in the investigation, the zero shift of the other two being discarded because of erratic behavior. The largest deviation of the AB-7 gages from ideal performance then was in the gage-to-gage variation of the zero shift which was apparently dependent on small variations in gage construction and installation.

These tests were concerned with uniaxial stresses. If more complicated states of stress are of interest, the measuring gages must be arranged in rosettes. In such cases, the stresses can be calculated by the applicable rosette formula if the net strain is used for each arm of the rosette. Reference 5 presents detailed information on the use of rosette gages and shows that the transverse sensitivity is a small quantity. A confirmatory investigation at room temperature indicated that the transverse sensitivity of AB-7 strain gages could be neglected.

The AB-7 wire strain gages therefore have satisfactory characteristics for the measurement of stresses under conditions of uniform stress and temperature, provided that the strain gages are properly mounted on the specimen and are cured and subjected to several temperature cycles and provided that the variation of the zero shift with temperature is determined for each individual gage. A complete stress-strain curve of the type shown in figure 1 is not necessary for each gage since the variation of elastic modulus with temperature can be obtained from any suitable source. In many tests, calibration of all of the gages mounted on the specimen may be impractical, and in such cases, an average zero shift can be used if accuracy can be sacrificed. The present investigation shows, however, that the use of an average zero shift would have given errors up to 1 ksi.

MEASUREMENT OF THERMAL STRESSES IN THE TEST PANEL

The tests described in the preceding section showed that the AB-7 gages had satisfactory characteristics for the measurement of thermal stresses under simple states of temperature and stress. The

suitability of the gages for the measurement of thermal stresses under more complicated conditions was therefore investigated by means of a test panel designed to provide a two-dimensional distribution of thermal stress under steady-state conditions. A simple configuration, arranged for experimental convenience, was chosen so that the accuracy of the experimental measurements could be verified by comparison with a theoretical solution. This configuration was also suitable for an experimental and theoretical investigation of thermal buckling of plates (ref. 6).

A flat, rectangular plate of $\frac{1}{4}$-inch-thick 75S-T6 aluminum alloy, measuring 24 by 36 inches, to which apparatus was attached for inducing a steady-state temperature gradient and measuring the resultant temperatures and stresses (figs. 4 and 5) was used. The temperature gradient was induced in the plate by heating its longitudinal center line and cooling its longitudinal edges. The heat was supplied by Nichrome wire imbedded in porcelain cement and was removed by water flowing through two plastic tubes glued to the plate. The size and material of the attached apparatus were such that negligible resistance was offered to thermal expansion of the plate. The sides and ends of the plate were insulated with asbestos (see fig. 4) to minimize heat loss through these surfaces and to insure that the instrumentation was at the same temperature as the plate. The flow of cooling water was controlled so that the temperature distribution was symmetrical about the longitudinal center line and essentially constant in the longitudinal direction. No measurable temperature variation occurred through the thickness of the plate.

Since the temperature distribution, and hence the stress distribution, was symmetrical about both center lines of the plate, strain gages were mounted on only one quadrant of the panel. At each point where strain measurements were taken, three AB-7 strain gages were arranged in a fan rosette and a similar group of strain gages was mounted on the reverse side. Iron-constantan thermocouples were mounted at the center of each fan on one side of the plate.

The thermal stresses induced in the plate tended to deform it out of its plane, a combined bending-buckling phenomenon associated with the initial imperfections of the plate. Since the present tests were concerned with plane stresses, this deformation was minimized by mounting the plate in a jig designed to provide the required restraint without introducing extraneous stresses. To further insure that the experimental stresses would closely approximate a state of plane stress, the readings of strain gages on opposite sides of the plate were averaged before the stresses were computed.

Three tests were made and in each the panel was heated until the temperature distribution stabilized; then the strain gages were read. The strain and temperature data were processed as follows:

(1) The temperature distribution was plotted and the average temperature of each strain gage determined.

(2) The zero shift of each gage was determined from its calibration curve.

(3) The net strain of each gage was obtained by subtracting its zero shift from its total strain.

(4) The net strains were plotted and the corrected net strains at the common point of each rosette were interpolated. This correction was necessary to obtain accurate results because a large strain gradient existed over some areas of the panel and the three gages of the rosette were necessarily located some distance apart.

(5) The corrected net strains from gages on opposite sides of the plate were averaged to get the midplane strain.

(6) The three stresses at each point (direct stresses in longitudinal and transverse directions and the shear stress) were computed from the three corrected net strains and the known properties of the material.

(7) The resulting stresses were then adjusted to a temperature difference of 150° F between the center line and longitudinal edges of the plate by assuming that the stresses were a linear function of the temperature difference. This adjustment was made to provide a common basis for comparing the three tests which were made at different temperature differences. Actually, the stresses do not vary linearly with temperature difference because of the changes in material properties; however, in the temperature range of the tests, the departure from linearity was very small because the decrease in the modulus of elasticity with temperature increase was offset by the increase in the coefficient of thermal expansion with temperature increase.

The results are shown in figures 6 to 9, in which the experimental results are compared with the theoretical results described in the next section. Figure 6 shows the transverse temperature distribution obtained at all longitudinal stations. Figure 7(a) shows the transverse distribution of the longitudinal direct stress at each of the transverse stations, and figure 7(b) shows the longitudinal distribution of the longitudinal direct stress at each of the longitudinal stations. Similarly, the shear stresses are shown in figures 8(a) and 8(b) and the transverse direct stresses are plotted in figures 9(a) and 9(b). The experimental points shown are the average of the three tests; separate points are not shown for each test since in most cases they are too close together to be easily distinguishable.

CALCULATION OF THERMAL STRESSES IN THE TEST PANEL

The stress distribution in the test panel was calculated by application of the theory of elasticity to provide a theoretical check on the measured stresses. The analysis is simplified by assuming that the test panel is a thin, flat, rectangular plate which is in a state of plane stress and which does not buckle out of its original plane and that the properties of the material are constant in the temperature range of interest.

The plate is free to expand in all directions; no external loads are applied; and all internal stresses are caused by a nonuniform temperature distribution. Pertinent dimensions and the coordinate system of such a plate are shown in figure 10 and the temperature distribution is shown in figures 6 and 11.

An exact solution of this problem can be obtained in the form of an infinite series. Such a solution, however, is inconvenient to evaluate numerically, and an approximate solution which is developed in the appendix is sufficiently accurate for general verification of the test results. Such an approximate solution is based on the assumption that the variation of the longitudinal direct stress σ_x in the transverse direction is the same as that given by the analysis of a very long plate in reference 7. The transverse distribution of shear stress τ_{xy} and the transverse distribution of direct stress σ_y are determined from the longitudinal direct stresses σ_x, equilibrium equations, and the stress-free boundary conditions on the longitudinal edges. The longitudinal variations of these stresses are obtained by application of the principle of minimum complementary energy.

The dimensions, temperature difference, and material properties used are

$$a = 18 \text{ in.}$$

$$b = 12 \text{ in.}$$

$$T_1 = 150^\circ \text{ F}$$

$$E = 10.4 \times 10^6 \text{ psi}$$

$$\alpha = 12.7 \times 10^{-6} \frac{\text{in.}}{\text{in.-}^\circ\text{F}}$$

and the results of the theoretical analysis of the test panel are

$$\sigma_x = 1651(y - 6)\left[1 - 0.0987 \sinh(0.1759x)\sin(0.0923x) - 0.1528 \cosh(0.1759x)\cos(0.0923x)\right]$$

$$\tau_{xy} = 82.55(y^2 - 12y)\left[0.0326 \cosh(0.1759x)\sin(0.0923x) + 0.3600 \sinh(0.1759x)\cos(0.0923x)\right]$$

$$\sigma_y = 2.752(y^3 - 18y^2 + 864)\left[0.2750 \sinh(0.1759x)\sin(0.0923x) - 0.6634 \cosh(0.1759x)\cos(0.0923x)\right]$$

$$(0 \leqq x \leqq 18;\ 0 \leqq y \leqq 12)$$

These equations give the stresses in the first quadrant; the stresses in the other quadrants can be obtained by noting that the direct stresses σ_x and σ_y are symmetrical and the shear stress τ_{xy} is antisymmetrical about both the longitudinal and transverse center lines.

RESULTS AND DISCUSSION

Temperature Distribution

The temperature increase of the instrumented quadrant of the test panel is shown in figure 6. The transverse distribution is shown for only one station; the others are not shown since they are identical. The temperature of the panel when the test began (80° F) was the temperature at which the initial gage readings were taken and thus is the temperature at which the thermal stresses were assumed to be zero.

The straight line drawn through the test points is the temperature distribution used to calculate the theoretical thermal stresses and corresponds to simple conduction between a concentrated heat source along the longitudinal center line and a concentrated heat sink along each longitudinal edge. The temperature difference shown between the center line and the edge is 150° F. The actual temperature distribution, given

by the test points, varied slightly from a straight line because of the finite area of the source and sink and because of heat loss through the sides and ends of the plate, but the measured points are within a few degrees of the straight line.

Longitudinal Direct Stresses σ_x

The longitudinal direct stresses induced in the plate by the temperature distribution of figure 6 are shown in figure 7. In figure 7(a) the transverse distribution of calculated and measured stresses is shown for four stations, and in figure 7(b) the same data are replotted to show the longitudinal distribution at three stations. The stresses are shown for only one quadrant of the plate, but the complete distribution is symmetrical about both center lines.

The results show that the hot parts of the plate near the longitudinal center line ($y = 0$) are in compression and the cold parts near the longitudinal edges ($y = 12$) are in tension, as would be expected, since the cold parts restrain the greater expansion of the hot parts. The theoretical results shown are seen to be in good agreement with the test data.

Shear Stresses τ_{xy}

The shear stresses induced in the plate are shown in figure 8, in which the presentation is similar to that in figure 7. Again the stresses are shown for only one quadrant of the plate, but in this case the complete distribution is antisymmetrical about both center lines if a uniform sign convention is used for shear stresses. The agreement between calculated and measured shear stresses is fairly good but not so good as for the longitudinal direct stress.

Transverse Direct Stresses σ_y

The transverse direct stresses induced in the plate are shown in figure 9 where the presentation is similar to that in figures 7 and 8. Results are shown for only one quadrant, but the complete distribution is symmetrical about both center lines. The agreement between calculated and measured values again is not so good as for the longitudinal direct stress.

Agreement Between Theory and Experiment

The general agreement between the measured and computed stresses is satisfactory with the difference being less than 1/2 ksi for all test points except one. Both the test data and theory are subject to inaccuracies, the magnitudes of which are not precisely known. The test and theory, however, mutually support one another and are of about the same order of accuracy, with the measurements probably being more accurate than the theoretical values. The fact that good agreement exists between calculated and measured longitudinal direct stresses and only fair agreement between calculated and measured transverse direct and shear stresses can be attributed to the errors introduced by the approximate analysis rather than errors in measurements.

A long thin plate subjected to a temperature distribution that is symmetrical about the longitudinal center line and independent of the distance along the plate length is analyzed in reference 7 and is shown to have induced longitudinal direct stresses σ_x but no transverse direct stresses σ_y or shear stresses τ_{xy}. In a short plate, such as investigated in the present paper, the condition that the edge stresses vanish necessitates the modification of the longitudinal direct stresses and introduces transverse direct stresses and shear stresses into the problem.

In the approximate analysis of the present paper the transverse variation of the longitudinal direct stress given by the long-plate solution is assumed to be valid for short plates and a correction is determined for the longitudinal variation of these stresses by the principle of minimum complementary energy. Since the long-plate solution does not involve transverse direct stresses and shear stresses, the corrected longitudinal direct stresses can be expected to be nearer the true values than the transverse direct stress σ_y and the shear stress τ_{xy} which are themselves corrections. Additional accuracy could be obtained by making additional corrections; however, the analysis used is estimated to be within 1/2 ksi (± 5 percent of the maximum calculated stress) of the exact solution in the region where the stresses were measured. Since this is of the same order of magnitude as the experimental accuracy, a more refined theoretical approach is not required.

CONCLUDING REMARKS

A technique has been described for measuring thermal stresses with commercially available bonded resistance wire strain gages. In such applications, wire strain gages cannot be expected to yield as accurate results as in more conventional uses because the temperature changes are

large and there is no simple way to compensate for the many errors thus introduced. The largest deviation from ideal performance was in the gage-to-gage variation of the zero shift due to temperature changes which was apparently dependent on small variations in gage construction and installation. This difficulty was overcome in the technique described by measuring the zero shift of each gage after it was installed on the test specimen and cured by several cycles of temperature higher than that reached during the test. Such a procedure may be impractical in many cases, since it involves uniform heating of the complete test specimen over the entire temperature range of interest. If this calibration is impractical and accuracy will permit, an average value of the zero shift obtained from a separate test may be used. In this case, however, errors up to 1 ksi may be expected in the range of conditions investigated in this paper.

The technique described was applied to the measurements of thermal stresses induced in a flat plate subjected to a known steady-state temperature gradient. The stresses so measured were compared with an approximate theoretical solution and were found to be in satisfactory agreement, that is, within about ± 5 percent of the maximum calculated stress.

Langley Aeronautical Laboratory
National Advisory Committee for Aeronautics
Langley Field, Va., June 9, 1952

APPENDIX

DERIVATION OF APPROXIMATE FORMULAS FOR THERMAL-STRESS DISTRIBUTION

The rectangular plate shown in figure 10 is analyzed under the following conditions:

(1) The temperature distribution is uniform over the plate thickness and varies over the plate surface in the following manner:

$$T = T_0 + XY \tag{A1}$$

where X is a function of x only and Y is a function of y only. The uniform temperature distribution T_0 is superimposed on the plate without affecting the problem – that is, a uniform temperature distribution produces no thermal stresses because of the next condition.

(2) No external loads are applied and the plate is free to expand in all directions so that all stresses are due to the nonuniform temperature distribution.

The following assumptions are also made:

(1) The plate is thin and may be considered to be in a state of plane stress.

(2) The properties of the material do not vary with temperature and the stresses are within the elastic range.

It is convenient to introduce the Airy stress function Φ such that

$$\left.\begin{aligned} \sigma_x &= \frac{\partial^2 \Phi}{\partial y^2} \\ \tau_{xy} &= -\frac{\partial^2 \Phi}{\partial x\, \partial y} \\ \sigma_y &= \frac{\partial^2 \Phi}{\partial x^2} \end{aligned}\right\} \tag{A2}$$

The exact solution of the stated problem is then given by the function Φ that satisfies the following differential equation (ref. 7):

$$\nabla^4\Phi = -E\alpha\nabla^2T \tag{A3}$$

A solution of equation (A3) can be obtained in the form of an infinite series; however, such a solution is inconvenient to evaluate numerically. The type of series encountered may be visualized by noting that Φ is mathematically equivalent to the deflection of a rectangular plate of uniform thickness with clamped edges and under a lateral load proportional to ∇^2T.

It is further assumed that, as a first approximation, the Airy stress function Φ can be expressed as

$$\Phi = fg \tag{A4}$$

where f is a function of x only and g is a function of y only. Then

$$\left.\begin{aligned} \sigma_x &= fg'' \\ \tau_{xy} &= -f'g' \\ \sigma_y &= f''g \end{aligned}\right\} \tag{A5}$$

The primes indicate differentiation of the function (f or g) with respect to its assigned variable (x or y).

The problem is solved by selecting an appropriate function g and then using the principle of minimum complimentary energy to determine a function f that gives the best approximation to the exact solution of equation (A3). The degree of approximation involved is dependent upon the function g selected. A good selection is a function proportional to the stress function of an infinitely long plate ($a = \infty$) subject to the temperature distribution $T = Y$. In this case, the stress distribution is independent of x; therefore, equation (A3) requires that

$$g^{IV} \propto Y'' \tag{A6a}$$

or

$$g'' \propto Y + B_1 y + B_2 \tag{A6b}$$

Since, from equation (A5), σ_x is proportional to g'', the distribution of σ_x is proportional to the temperature distribution Y plus a linear distribution $B_1 y + B_2$ required to maintain thrust and moment equilibrium on the cross section. These results are the same as those obtained for an infinitely long plate by a somewhat different process in reference 7. The function g is obtained by integrating g'' twice and the two additional constants of integration are determined from conditions at the edges $y = \pm b$. This process is illustrated subsequently by a particular example. In the following paragraphs, the equations for determining f are developed with the assumption that g is some known function of y.

The complementary energy of a heated plate may be written as

$$U = \frac{1}{2E} \int_{-a}^{a} \int_{-b}^{b} \left[\sigma_x^2 + \sigma_y^2 - 2\mu\sigma_x\sigma_y + 2(1 + \mu)\tau_{xy}^2 + 2E\alpha T(\sigma_x + \sigma_y) \right] dx\, dy \tag{A7}$$

where the term involving αT expresses the strain energy resulting from thermal expansion. If equations (A1) and (A5) are substituted into equation (A7), the complementary-energy expression becomes

$$U = \frac{1}{2E} \int_{-a}^{a} \left\{ A_1 f^2 + A_2 f''^2 - 2\mu A_3 f f'' + 2(1 + \mu) A_4 f'^2 + 2E\alpha \left[(A_5 + A_6 X) f + (A_7 + A_8 X) f'' \right] \right\} dx \tag{A8}$$

where

$$A_1 = \int_{-b}^{b} g''^2 dy$$

$$A_2 = \int_{-b}^{b} g^2 dy$$

$$A_3 = \int_{-b}^{b} gg'' \, dy = \left[gg'\right]_{-b}^{b} - A_4$$

$$A_4 = \int_{-b}^{b} g'^2 dy$$

$$A_5 = T_0 \int_{-b}^{b} g'' \, dy = T_0 \left[g'\right]_{-b}^{b}$$

$$A_6 = \int_{-b}^{b} Yg'' \, dy$$

$$A_7 = T_0 \int_{-b}^{b} g \, dy$$

$$A_8 = \int_{-b}^{b} Yg \, dy$$

The complementary energy is now minimized by setting the first variation of U, obtained by the usual procedures of the calculus of variables, equal to zero. Since g is a known function of y, the result, after integration by parts, is

$$\delta U = \frac{1}{E}\int_{-a}^{a}\left\{A_1 f + A_2 f^{IV} - 2\left[A_4 + \mu\left(A_3 + A_4\right)\right] f'' + E\alpha\left(A_5 + A_6 X + A_8 X''\right)\right\}\delta f\, dx + \frac{1}{E}\left[\left\{\left[\mu A_3 + 2(1+\mu)A_4\right] f' - A_2 f''' - E\alpha A_8 X'\right\}\delta f\right]_{-a}^{a} + \frac{1}{E}\left[\left[A_2 f'' - \mu A_3 f' + E\alpha\left(A_7 + A_8 X\right)\right]\delta f'\right]_{-a}^{a} \tag{A9}$$

The terms under the integral sign yield the differential equation for the function f

$$A_2 f^{IV} - 2\left[A_4 + \mu\left(A_3 + A_4\right)\right] f'' + A_1 f = -E\alpha\left(A_5 + A_6 X + A_8 X''\right) \tag{A10}$$

The remaining terms set equal to zero are the boundary conditions. The problem as stated requires that the edges of the plate be stress-free, so that physically the boundary conditions are:

At $x = \pm a$,

$$\sigma_x = \tau_{xy} = 0 \tag{A11a}$$

and at $y = \pm b$,

$$\sigma_y = \tau_{xy} = 0 \tag{A11b}$$

Equations (A11a) require that f and f' vanish at $x = \pm a$, so that the requirements of the boundary terms of equation (A9) are satisfied. Equations (A11b) give boundary conditions which must be considered in the selection of g and require that, from equation (A8),

$$A_3 = -A_4 \tag{A12a}$$

$$A_5 = 0 \tag{A12b}$$

Equation (A12a) shows that the approximate solution is not dependent on Poisson's ratio μ, a result that is not surprising since the exact solution does not involve μ. The differential equation for f then becomes

$$A_2 f^{IV} - 2A_4 f'' + A_1 f = -E\alpha\left(A_6 X + A_8 X''\right) \tag{A13}$$

Equation (A13) is now solved for the temperature distribution shown in figure 11. This distribution, which does not vary with x, has a discontinuity along the x-axis and cannot be defined by a single, simple analytical expression. The stress distribution in the plate due to this temperature distribution is symmetrical about the plate center lines. The analysis can therefore be confined to the first quadrant of the plate. The temperature distribution in this quadrant is then given by

$$\left.\begin{aligned} X &= T_1 = \text{Constant} \\ Y &= 1 - \frac{y}{b} \\ T &= T_0 + T_1\left(1 - \frac{y}{b}\right) \end{aligned}\right\} \tag{A14}$$

The function g is found from the criterion of equation (A6b) and the requirement that the stress distribution is symmetrical about the plate center line; that is,

$$g'' \propto Y + B_2 = 1 - \frac{y}{b} + B_2 \tag{A15}$$

or, since an arbitrary constant can be removed without affecting the solution,

$$g'' = \frac{y}{b} + B_3 \tag{A16a}$$

Then

$$g' = b\left[\frac{1}{2}\left(\frac{y}{b}\right)^2 + B_3\,\frac{y}{b} + B_4\right] \tag{A16b}$$

and

$$g = b^2\left[\frac{1}{6}\left(\frac{y}{b}\right)^3 + \frac{1}{2}B_3\left(\frac{y}{b}\right)^2 + B_4\frac{y}{b} + B_5\right] \tag{A16c}$$

The boundary conditions of equation (A11b) should determine the constants of integration in equations (A16); however, only one quadrant is being analyzed and the conditions at $y = -b$ are not applicable. Conditions of symmetry are used instead — that is, σ_x and σ_y are made symmetrical about the x-axis. The boundary conditions required to define g are then

$$\left.\begin{aligned} g'(0) &= 0 \\ g(b) &= 0 \\ g'(b) &= 0 \end{aligned}\right\} \tag{A17}$$

in which case

$$g = \frac{b^2}{12}\left[1 - 3\left(\frac{y}{b}\right)^2 + 2\left(\frac{y}{b}\right)^3\right] \tag{A18}$$

Since Y and g are given by equations (A14) and (A18), the integrals A_1 to A_8 can be evaluated to determine the coefficients of equation (A13). After some simplification the result is

$$13b^4f^{IV} - 84b^2f'' + 420f = 420E\alpha T_1 \tag{A19}$$

The solution of equation (A19) can be written as follows:

$$f = E\alpha T_1\left(1 + C_1 \sinh k_1x \sin k_2x + C_2 \sinh k_1x \cos k_2x + C_3 \cosh k_1x \sin k_2x + C_4 \cosh k_1x \cos k_2x\right) \tag{A20}$$

where

$$k_1^2 = \frac{21 + \sqrt{1365}}{13b^2}$$

and

$$k_2^2 = \frac{-21 + \sqrt{1365}}{13b^2}$$

The boundary conditions of equation (A11a) determine the constants of integration, but conditions of symmetry may be used instead of the conditions at $x = -a$ since the analysis is confined to the first quadrant. The required relations are then:

$$\left.\begin{aligned} f'(0) &= 0 \\ f'''(0) &= 0 \\ f(a) &= 0 \\ f'(a) &= 0 \end{aligned}\right\} \qquad (A21)$$

The substitution of equation (A20) into equations (A21) gives four equations for the constants of integration C_1 to C_4 which may be solved to yield

$$\left.\begin{aligned} C_1 &= \frac{k_1 \sinh k_1 a \cos k_2 a - k_2 \cosh k_1 a \sin k_2 a}{k_1 \sin k_2 a \cos k_2 a + k_2 \sinh k_1 a \cosh k_1 a} \\ C_2 &= C_3 = 0 \\ C_4 &= -\frac{k_1 \cosh k_1 a \sin k_2 a + k_2 \sinh k_1 a \cos k_2 a}{k_1 \sin k_2 a \cos k_2 a + k_2 \sinh k_1 a \cosh k_1 a} \end{aligned}\right\} \qquad (A22)$$

The following expressions for the stresses can be obtained by substituting equations (A18) and (A20) into equations (A5):

$$\left.\begin{aligned}
\sigma_x &= \frac{E\alpha T_1}{2}\left(2\,\frac{y}{b} - 1\right)\left(1 + C_1 \sinh k_1 x \sin k_2 x + C_4 \cosh k_1 x \cos k_2 x\right) \\
\tau_{xy} &= -\frac{E\alpha T_1}{2} b\left[\left(\frac{y}{b}\right)^2 - \frac{y}{b}\right]\left(C_5 \sinh k_1 x \cos k_2 x + C_6 \cosh k_1 x \sin k_2 x\right) \\
\sigma_y &= \frac{E\alpha T_1}{2}\,\frac{b^2}{6}\left[2\left(\frac{y}{b}\right)^3 - 3\left(\frac{y}{b}\right)^2 + 1\right]\left(C_7 \sinh k_1 x \sin k_2 x + C_8 \cosh k_1 x \cos k_2 x\right)
\end{aligned}\right\} \quad (A23)$$

where

$$C_5 = C_1 k_2 + C_4 k_1$$

$$C_6 = C_1 k_1 - C_4 k_2$$

$$C_7 = C_1\left(k_1^2 - k_2^2\right) - 2C_4 k_1 k_2$$

$$C_8 = 2C_1 k_1 k_2 + C_4\left(k_1^2 - k_2^2\right)$$

REFERENCES

1. Heldenfels, Richard R.: The Effect of Nonuniform Temperature Distributions on the Stresses and Distortions of Stiffened-Shell Structures. NACA TN 2240, 1950.

2. Heldenfels, Richard R.: A Numerical Method for the Stress Analysis of Stiffened-Shell Structures Under Nonuniform Temperature Distributions. NACA Rep. 1043, 1951. (Supersedes NACA TN 2241.)

3. Day, Emmett E.: Characteristics of Electric Strain Gages at Elevated Temperatures. Proc. Soc. Exp. Stress Analysis, vol. IX, no. 1, 1951, pp. 141-150.

4. Heimerl, George J., and Roberts, William M.: Determination of Plate Compressive Strengths at Elevated Temperatures. NACA Rep. 960, 1950. (Supersedes NACA TN 1806.)

5. Baumberger, R., and Hines, F.: Practical Reduction Formulas for Use on Bonded Wire Strain Gages in Two-Dimensional Stress Fields. Proc. Soc. Exp. Stress Analysis, vol. II, no. 1, 1944, pp. 113-127.

6. Gossard, Myron L., Seide, Paul, and Roberts, William M.: Thermal Buckling of Plates. NACA TN 2771, 1952.

7. Timoshenko, S., and Goodier, J. N.: Theory of Elasticity. Second ed., McGraw-Hill Book Co., Inc., 1951, pp. 398-437.

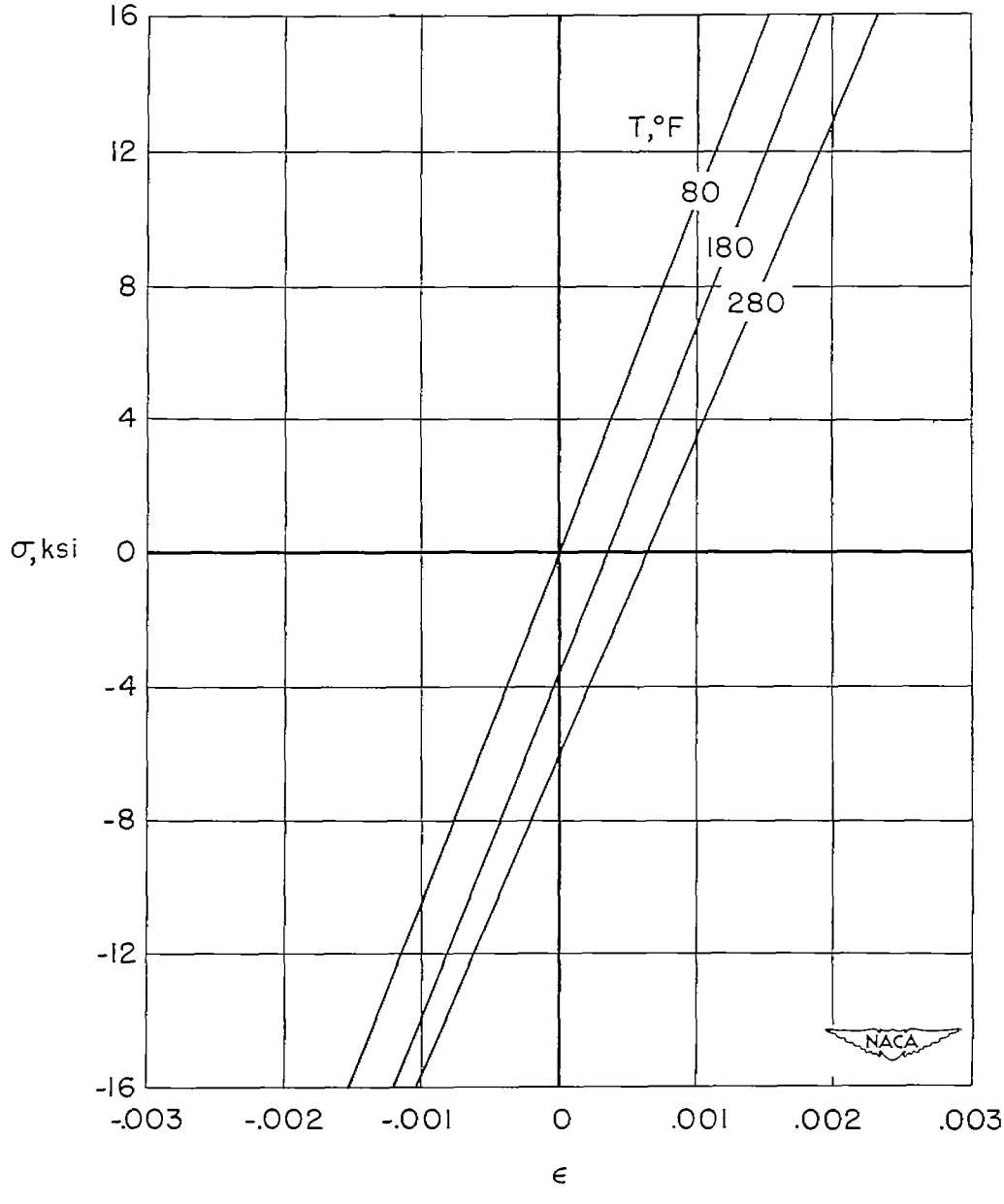

Figure 1.- Typical stress-strain curves for wire strain gages mounted on 75S-T6 aluminum alloy.

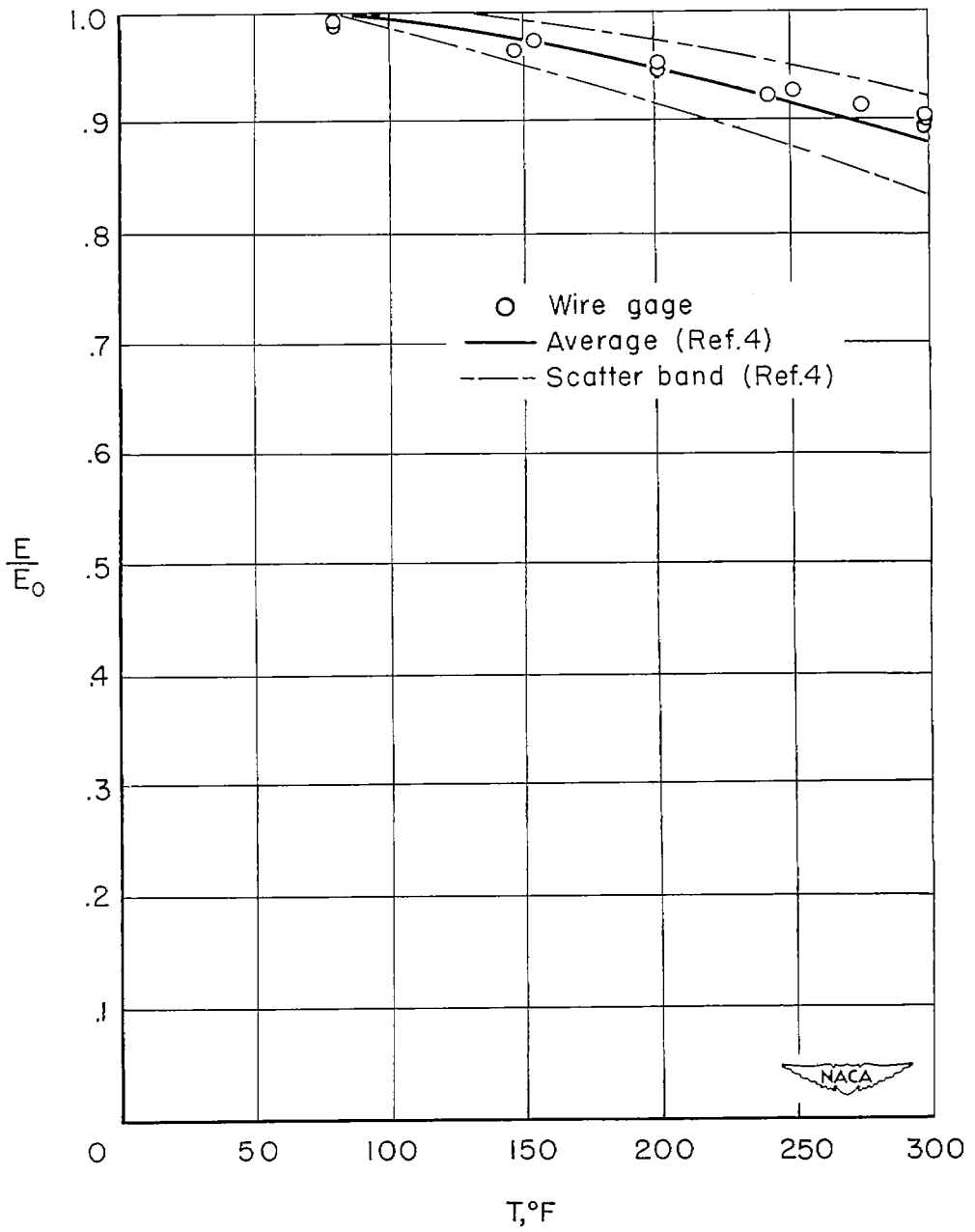

Figure 2.- Ratio of modulus of elasticity at elevated temperature to that at room temperature for 75S-T6 aluminum alloy.

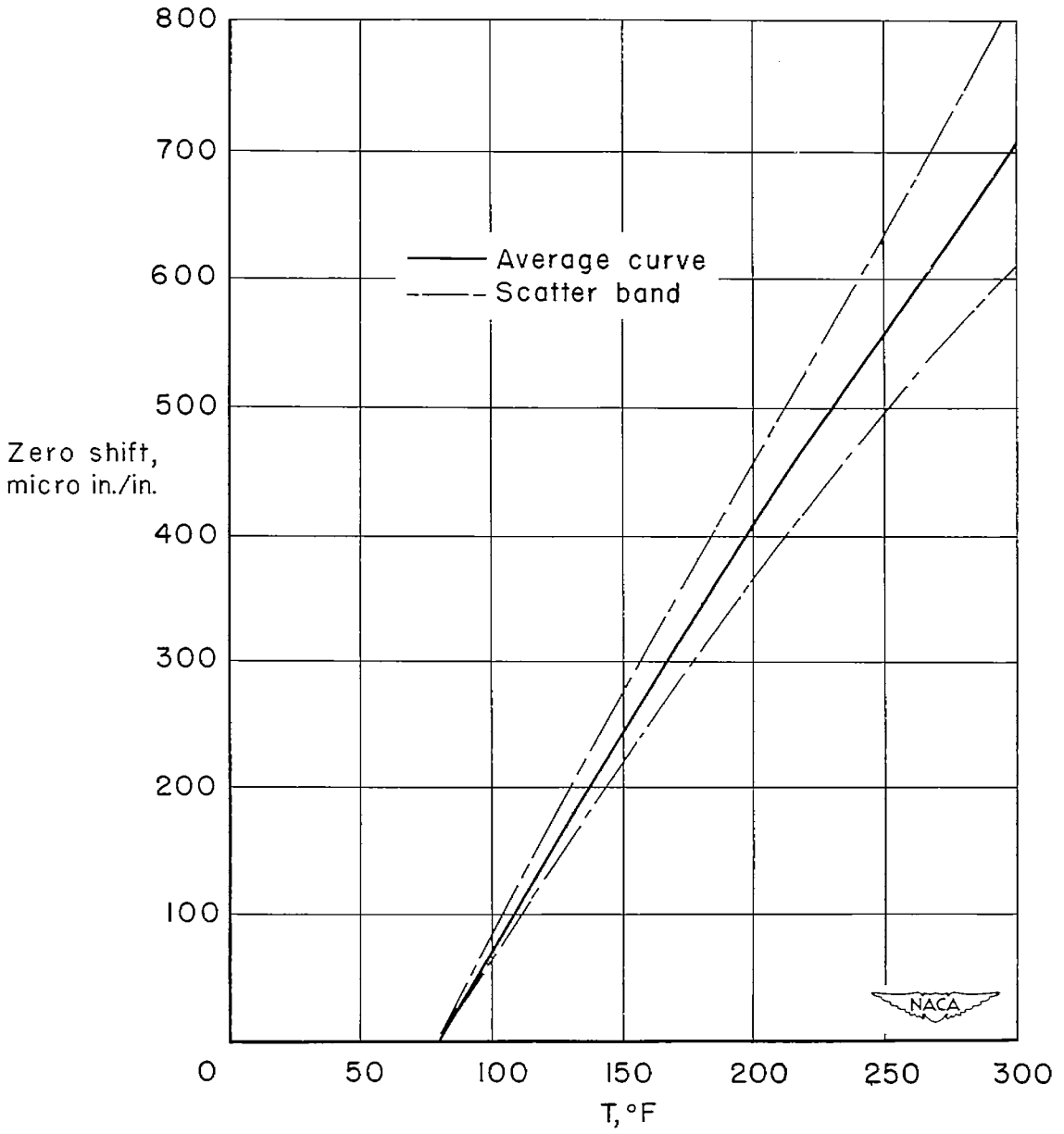

Figure 3.- Zero shift, due to temperature change, of 70 wire strain gages mounted on 75S-T6 aluminum alloy.

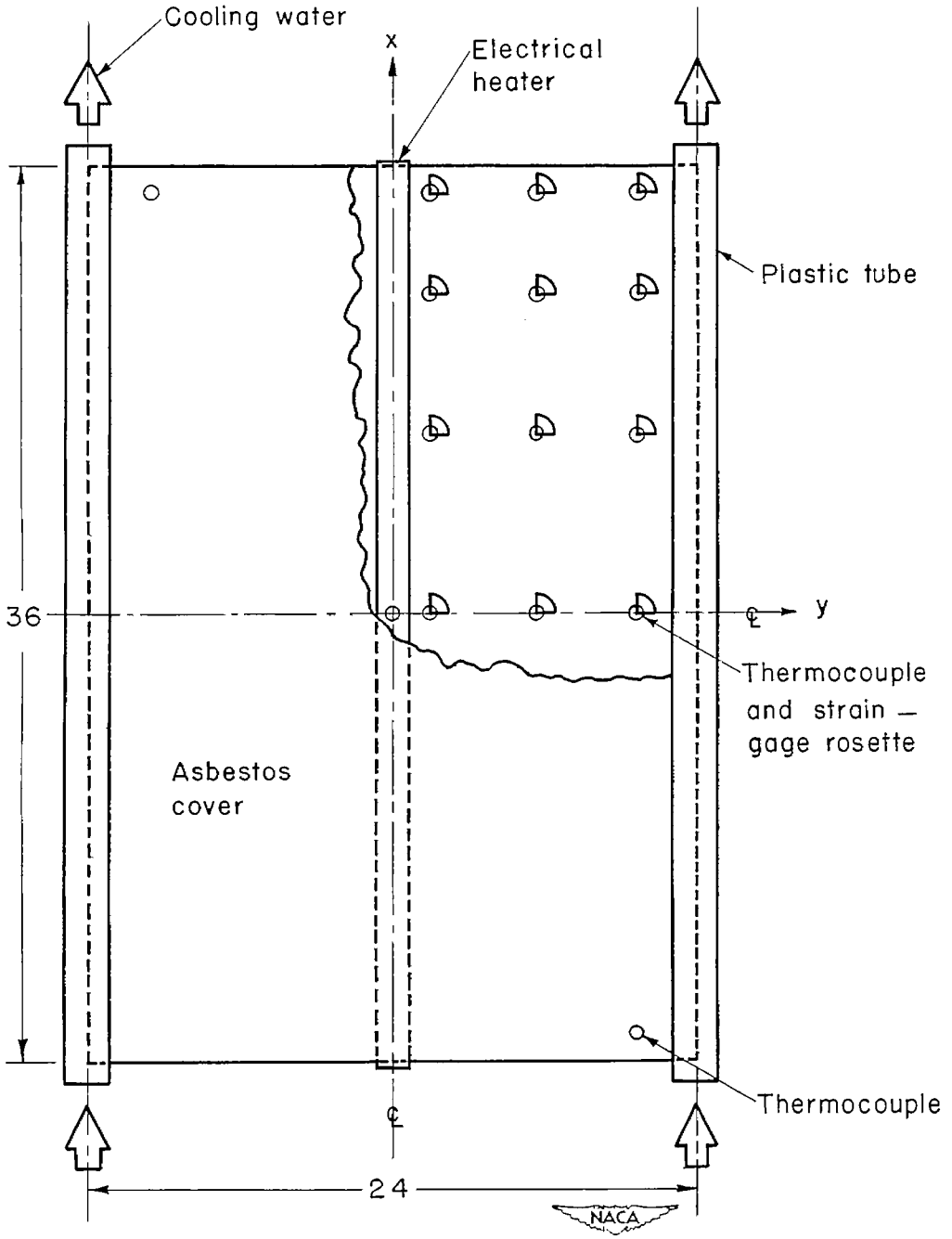

Figure 4.- Sketch of thermal-stress test specimen.

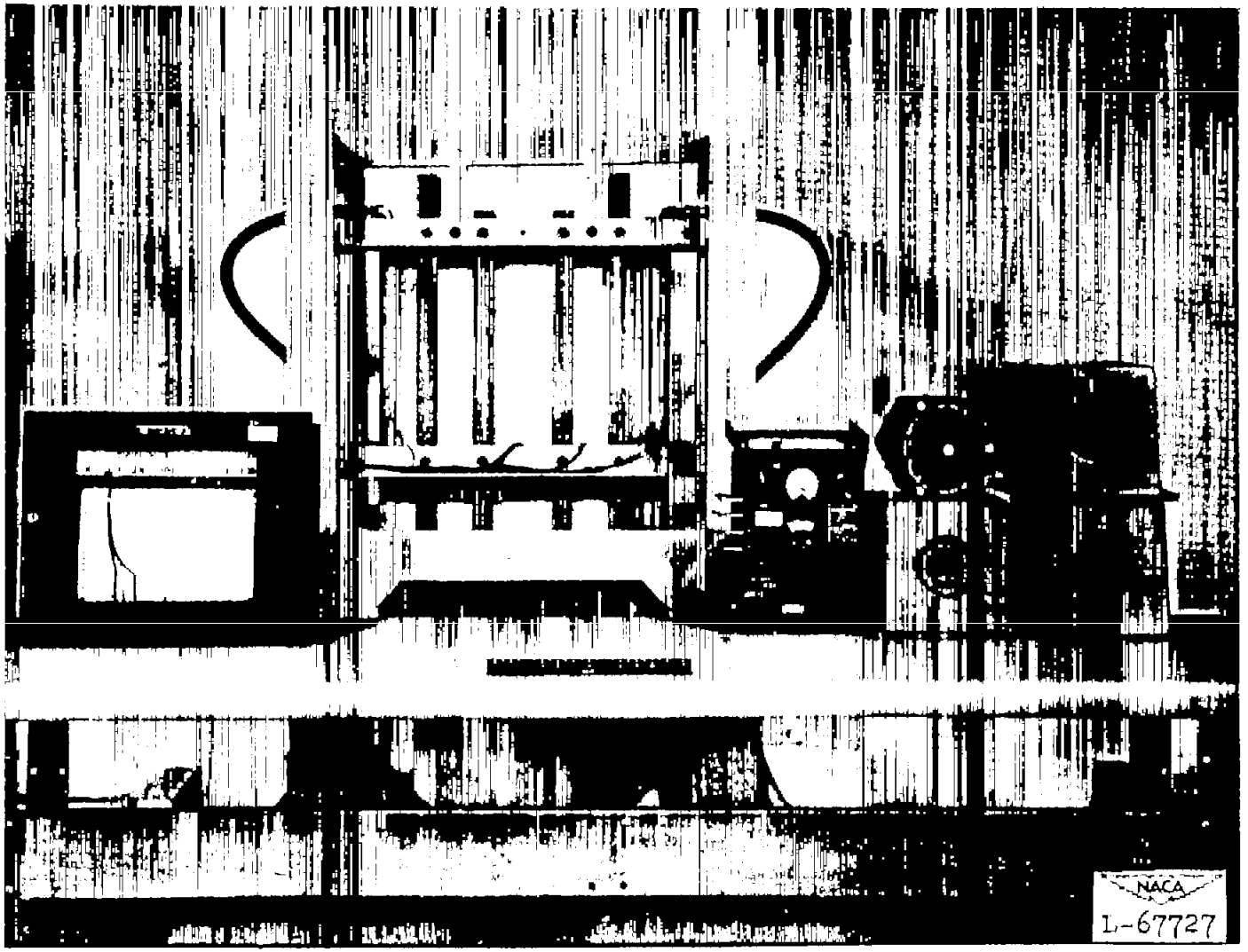

Figure 5.- Photograph of test setup.

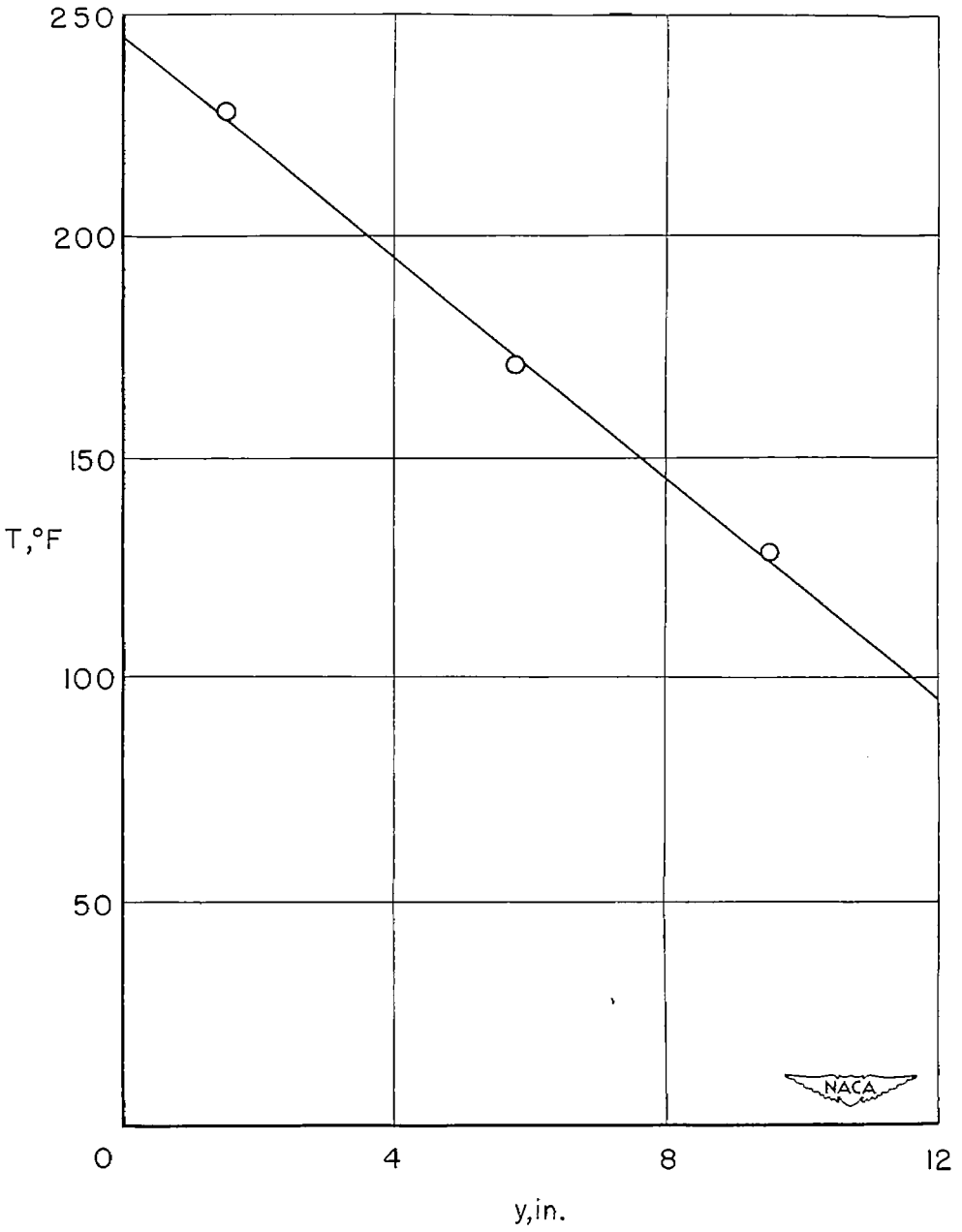

Figure 6.- Transverse temperature distribution.

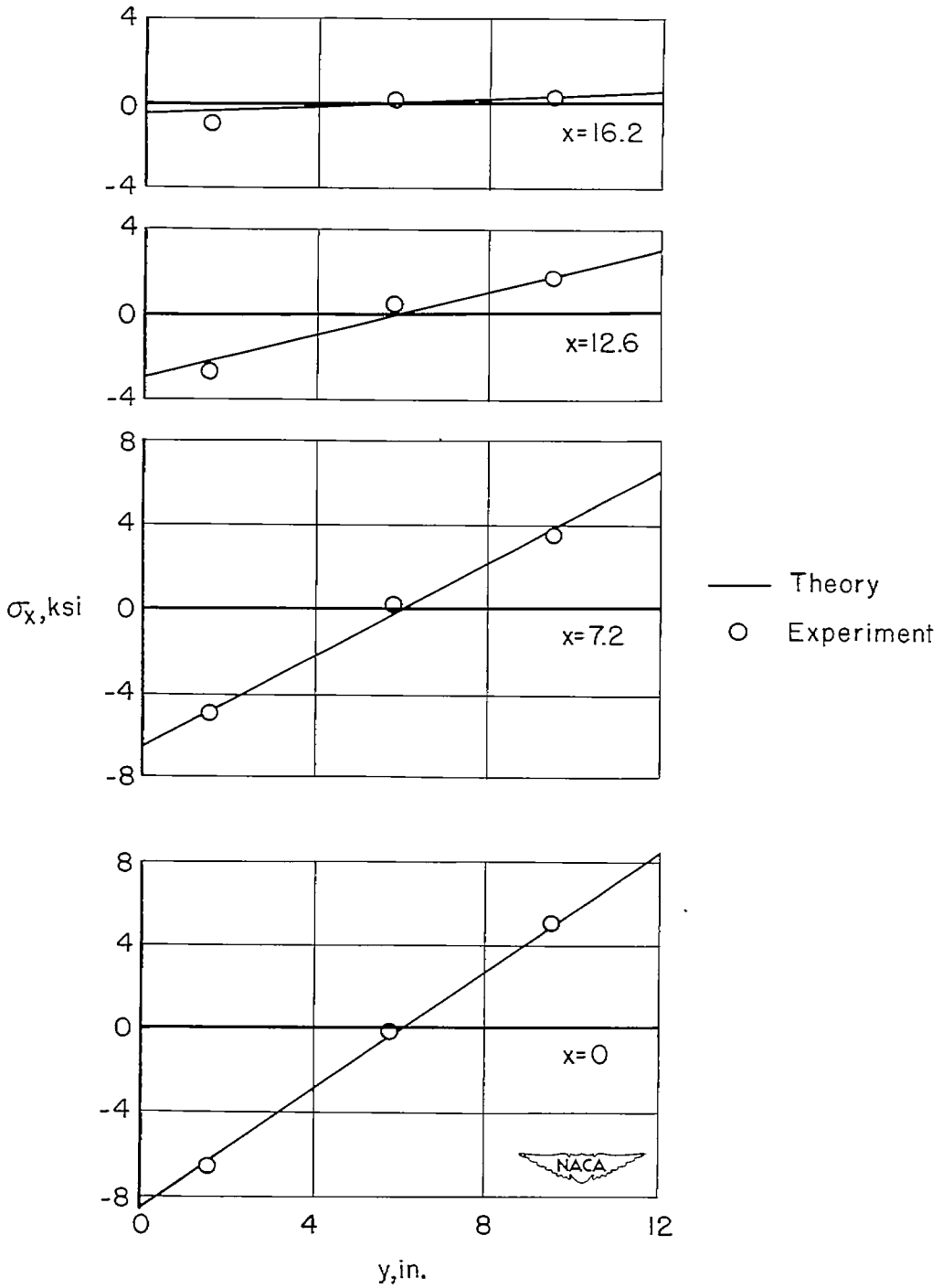

(a) Transverse distribution.

Figure 7.- Longitudinal direct stresses induced in test specimen by the temperature distribution of figure 6.

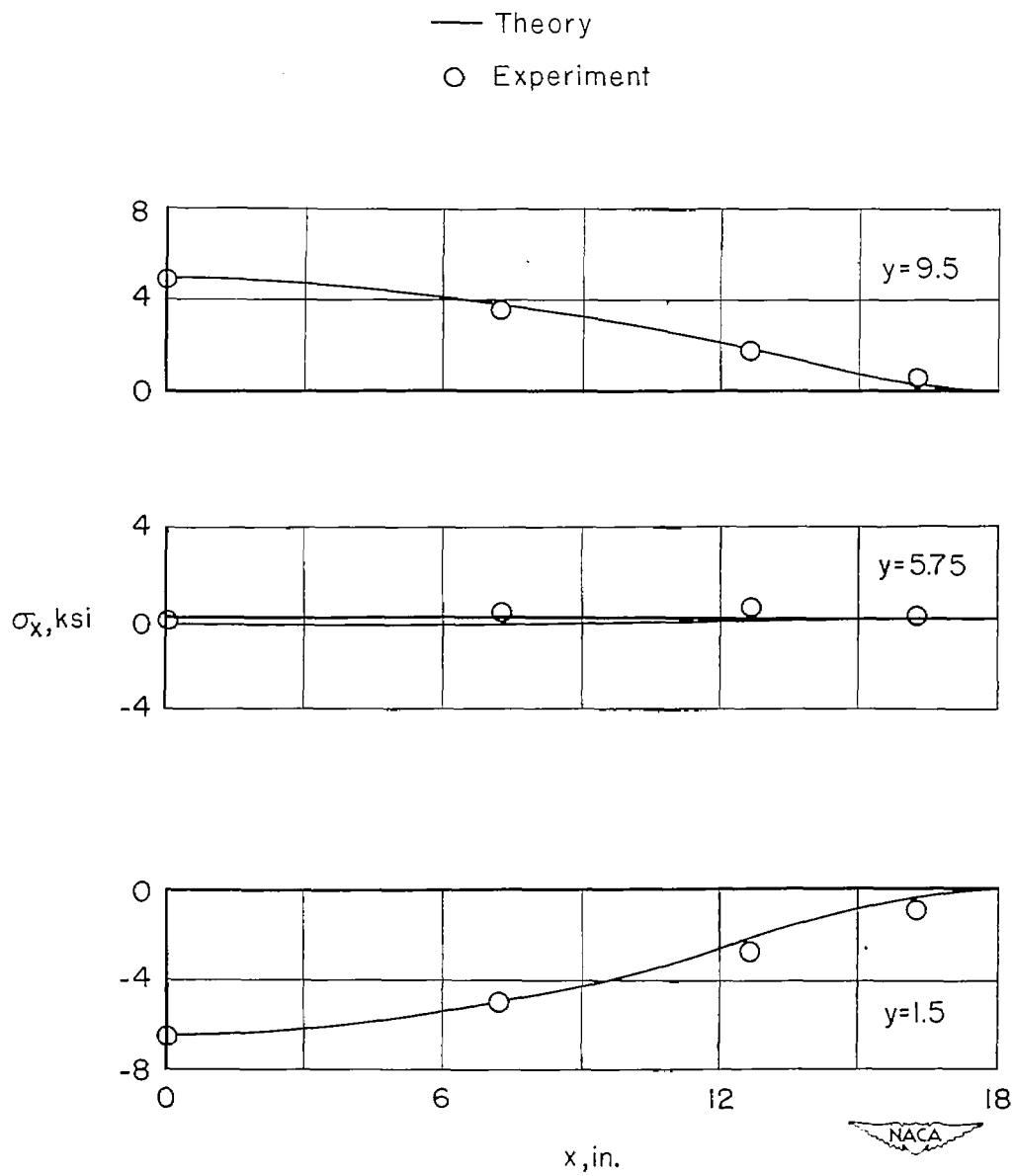

(b) Longitudinal distribution.

Figure 7.- Concluded.

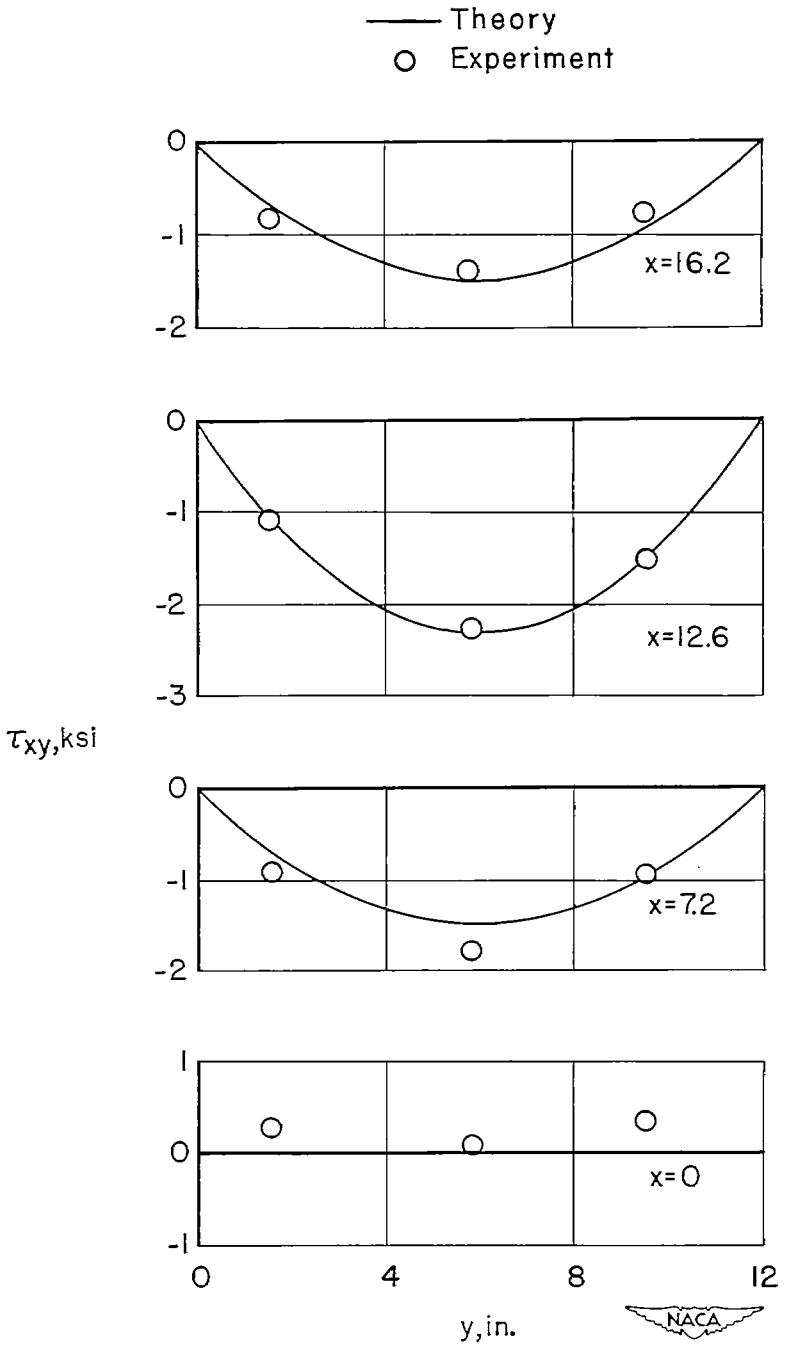

(a) Transverse distribution.

Figure 8.- Shear stresses induced in test specimen by the temperature distribution of figure 6.

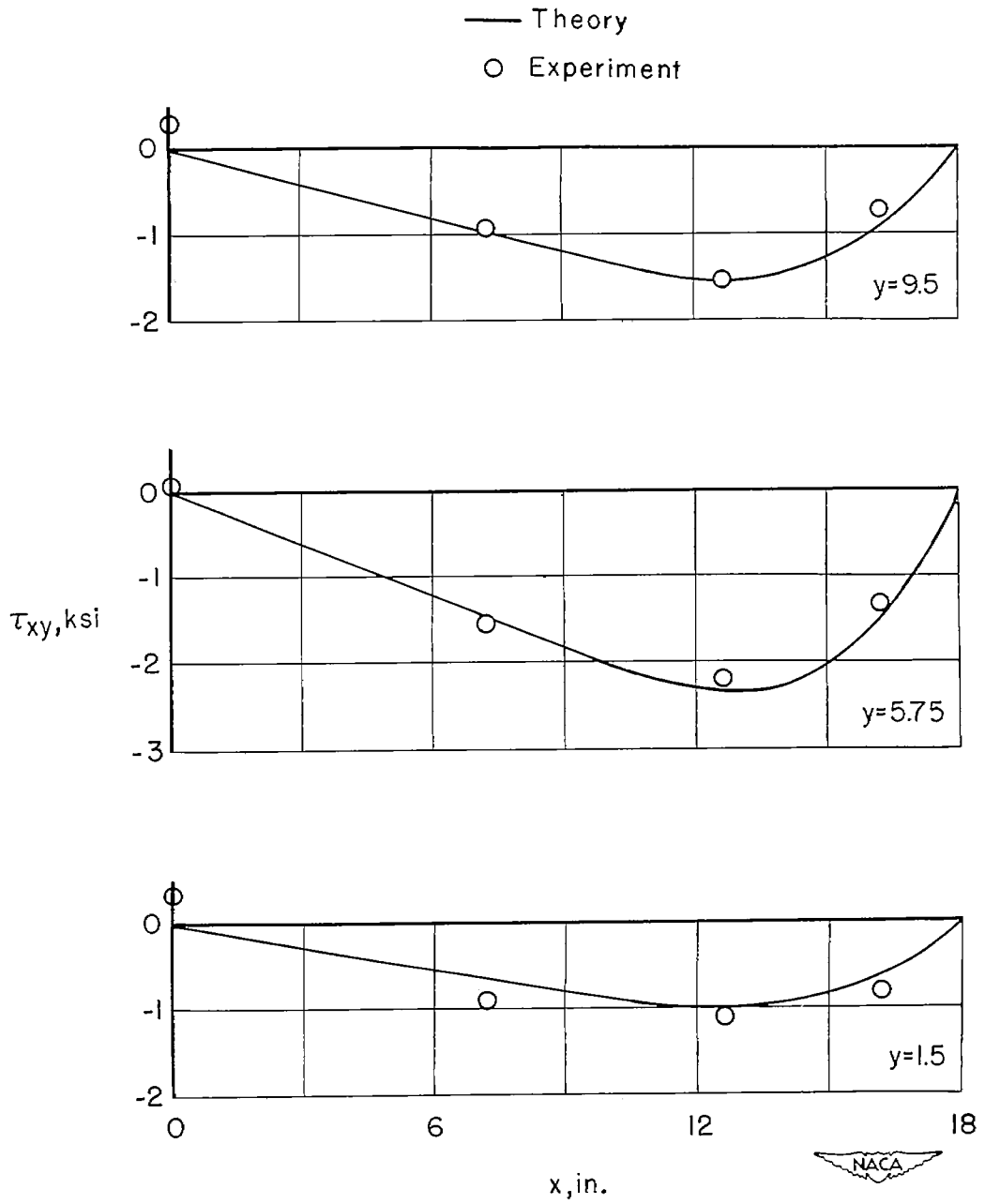

(b) Longitudinal distribution.

Figure 8.- Concluded.

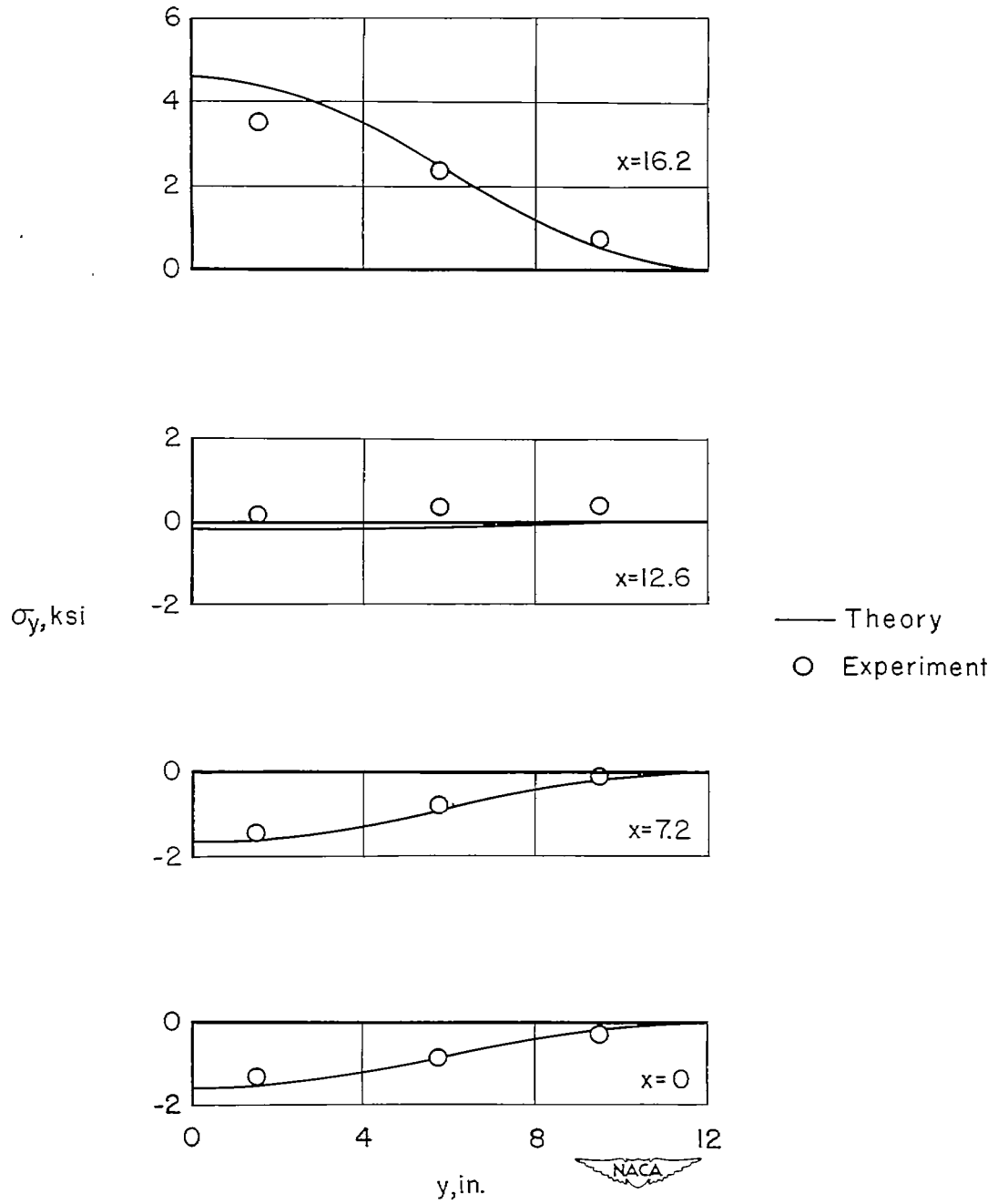

(a) Transverse distribution.

Figure 9.- Transverse direct stresses induced in test specimen by the temperature distribution of figure 6.

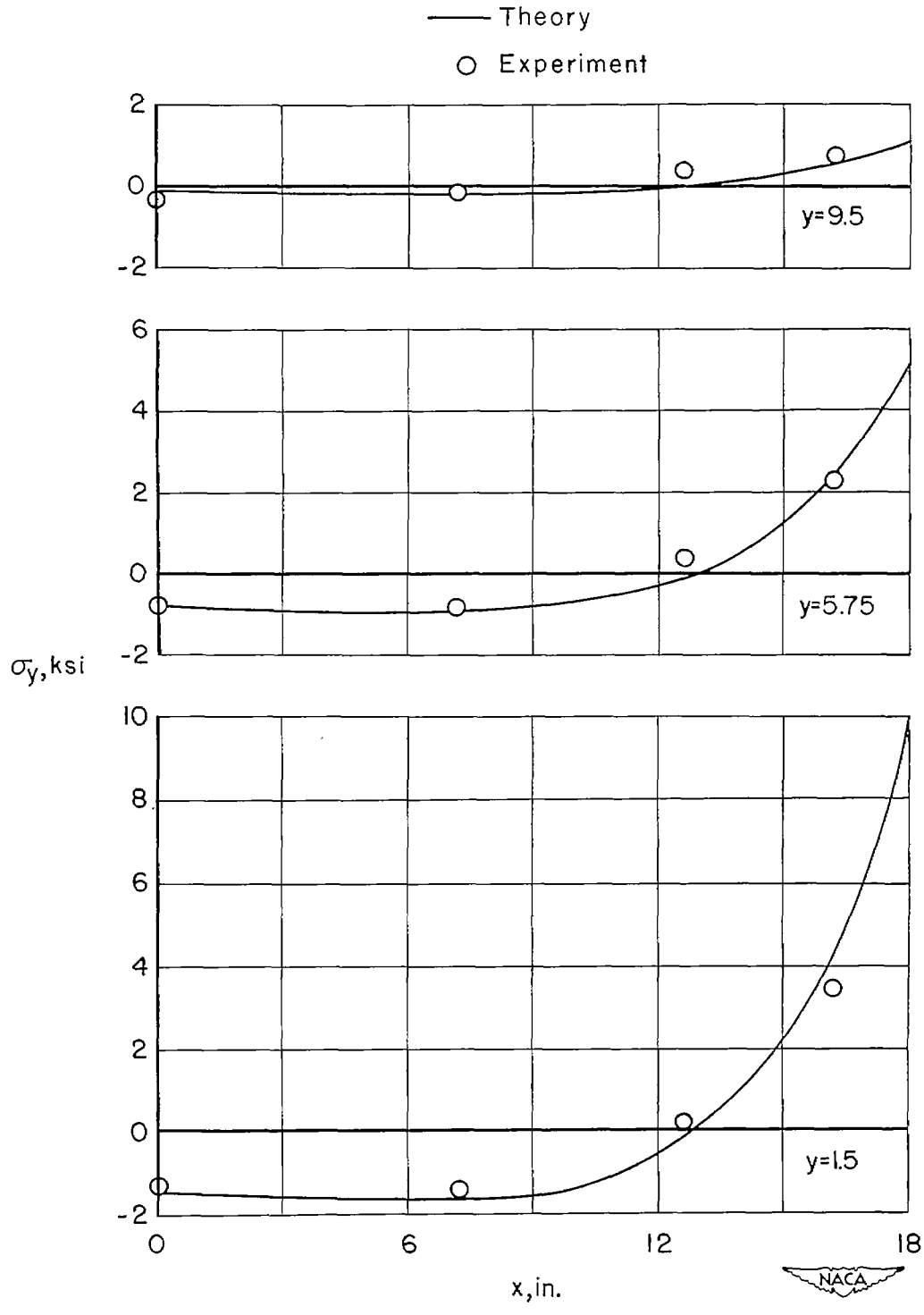

(b) Longitudinal distribution.

Figure 9.- Concluded.

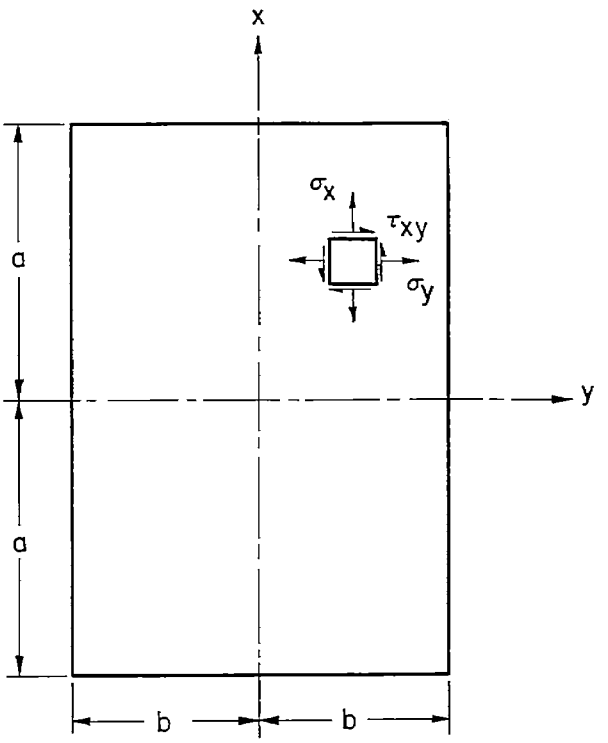

Figure 10.- Dimensions and coordinate system of plate analyzed in the appendix.

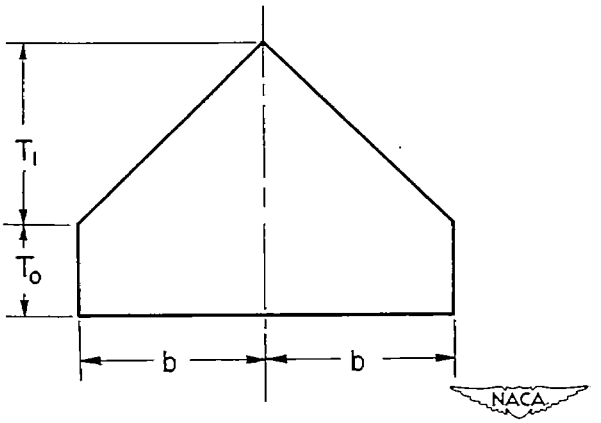

Figure 11.- Transverse temperature distribution on plate analyzed in the appendix.